Journal of Nuclear Materials 543 (2021) 152600

Contents lists available at ScienceDirect

Journal of Nuclear Materials

journal homepage: www.elsevier.com/locate/jnucmat

Thermal annealing and transformation of dimer *F* centers in neutron-irradiated Al_2O_3 single crystals

E. Shablonin[a], A.I. Popov[a,b], G. Prieditis[a], E. Vasil'chenko[a,b], A. Lushchik[a,*]

[a] Institute of Physics, University of Tartu, W. Ostwald Str. 1, 50411 Tartu, Estonia
[b] Institute of Solid State Physics, University of Latvia, Kengaraga 8, Riga LV-1063, Latvia

ARTICLE INFO

Article history:
Received 30 April 2020
Revised 21 September 2020
Accepted 12 October 2020
Available online 20 October 2020

Keywords:
Irradiation by fast neutrons
Dimer F-type centers, Radiation induced optical absorption
Thermal annealing
α-Al_2O_3

ABSTRACT

The precise study of the thermal annealing of the F_2-type dimer defects, being under discussion in the literature for a long time and responsible for the number of absorption bands below 4.5 eV, has been performed in corundum single crystals irradiated by fast neutrons with a fluence of 6.9×10^{18} n/cm^2. The Gaussian components of the radiation-induced optical absorption with the maxima at 4.08, 3.45 and 2.75 eV have been considered as a measure of the F_2, $F_2^+$and F_2^{2+}centers, respectively. In contrast to the *F* and F^+ centers, the concentration of which continuously decreases at the sample heating up to 1100 K, the concentration of dimer defects with different charge states passes the increasing stages above 500 K starting from the F_2^{2+}centers. The tentative mechanisms of such rise of the F_2^{2+}centers as well as of the subsequent transformation/rise of dimer centers, $F_2^{2+} \rightarrow F_2^+ \rightarrow F_2$at 650-800 K are considered. The possible sources of carriers needed for the recharging of dimer centers are also analysed on the basis of thermally stimulated luminescence measurements up to ~850 K.

1. Introduction

Aluminium oxide (α-Al_2O_3) possesses a variety of fascinating properties allowing its use for different technological applications. In particular, because of high resistance to fast neutrons, rather low swelling and ability to maintain mechanical and electrical integrity, α-Al_2O_3 single crystals and polycrystalline transparent ceramics are widely used for fission-based energetics and are in the list of promising diagnostics/window materials for deuterium-tritium fusion reactors [1-3]. On the other hand, a specially treated alumina (so-called anion-deficient α-Al_2O_3) is the basis of highly sensitive luminescent detectors of ionizing radiation (see, e.g., [4,5] and references therein).

The processes of radiation damage under irradiation of α-Al_2O_3 crystals by fast fission neutrons, energetic electrons and swift heavy ions have been investigated for many years [1,6–17]. In general, tolerance of a functional material to intentional irradiation is mainly determined by the accumulation of primary lattice point defects – vacancy-interstitial Frenkel pairs. The optical absorption/emission bands related to the anion-vacancy-related elementary Frenkel defects – the F^+ and *F* centers (one or two electrons trapped by an oxygen vacancy) as well as their simplest aggregates, F_2 dimers (two adjacent oxygen vacancies) in different charge states have been revealed and thoroughly studied in the irradiated or additively colored (thermochemically reduced) Al_2O_3 crystals [7-12]. Particular emphasis has been also paid to thermal annealing of *F*- and F_2-types of radiation defects in α-Al_2O_3 [6,9,11,12,17], as well as to the analysis of their annealing kinetics [17,18] and the simulation of the migration of oxygen interstitials, a mobile component in a thermally stimulated recombination of complementary Frenkel defects [19-21].

By the modern concepts, the elastic collisions of incident energetic particles (neutrons, light and heavy ions, electrons) with atoms/nuclei of materials mainly determine the formation of radiation damage in wide-gap metal oxides. The displacement (knock-on, impact) creation mechanism completely describes the creation of Frenkel defects by fast neutrons [6]. On the other hand, swift heavy ions provide extremely high density of electronic excitations within cylindrical tracks, and, in addition to collision cascades, ionization losses can contribute to radiation damage of metal oxides as well (see [15,22,23] and references therein). Note that in contrast to alkali halides (see recent review [24]), more complex electronic excitation related mechanisms of Frenkel defect creation should be considered [15,23].

The present study is devoted to the precise measuring of the thermal annealing of the absorption bands related to dimer F_2-type centers created in α-Al_2O_3 single crystals under fast neu-

* Corresponding Author. Institute of Physics, University of Tartu, W. Ostwald Str. 1, 50411 Tartu, Estonia
E-mail addresses: popov@latnet.lv (A.I. Popov), aleksandr.lushchik@ut.ee (A. Lushchik).

https://doi.org/10.1016/j.jnucmat.2020.152600
0022-3115/

tron irradiation. Special attention is paid to possible mechanisms of the transformation between F_2-type centers with different charge states (F_2, $F_2^+$and F_2^{2+}), which are being implemented at temperatures above 650 K.

2. Experimental

Nominally pure α-Al_2O_3 single crystals were grown by means of the Czochralski method by Union Carbide Corporation. The crystals were irradiated by fission neutrons possessing energy higher than 0.1 MeV with a fluence about 6.9×10^{18} n/cm^2 at the Oak Ridge National Laboratory, while the sample temperature during irradiation did not exceed 60°C.

The spectra of optical absorption in ordinary spectral region of 1.5-6.5 eV were measured by a high-absorbance spectrometer JASCO V-660 with a double monochromator, while the measurements covering near vacuum ultraviolet (VUV, up to 8.5 eV) were performed using a VMR-2 vacuum monochromator and a hydrogen discharge light source. The difference between two absorption spectra sequentially measured at room temperature (RT) for a virgin crystal and the sample irradiated with fast fission neutrons was regarded as radiation-induced optical absorption (RIOA). In order to stay within experimental limits of optical density values (OD $\leq$ 4.0) in a whole spectral region, a 0.09-mm thickness sample was used; whereas the RIOA measurements in the responsibility region of the F_2-type dimer centers were performed for a thick sample, d = 0.37 mm. In both cases, about 8 × 8 mm^2 plates, both sides polished and parallel to the main c crystal axes, were used. The RIOA spectra were decomposed into Gaussian components connected with the creation of different radiation-induced structural defects.

The thermal annealing of radiation-induced damage in Al_2O_3 single crystals (i.e. recovering of the irradiated sample) was performed via the following stepwise procedure: the irradiated crystal was placed into a quartz reactor and heated to a certain temperature T_{pr} in an argon flowing atmosphere; kept at this fixed T_{pr} for about 10 min and then cooled down to RT by moving the reactor out of the furnace; finally, the RIOA of the sample preheated in a such way was measured at RT. Similarly, multiple "heating-cooling-measuring" cycles were carried out for the same sample under the same conditions with the consistent increase of T_{pr} by 15−40 K. Recently, the similar studies of radiation damage annealing have been also performed for cubic single crystals of MgO and $MgAl_2O_4$, the latter being an equimolar mixture of MgO and Al_2O_3 binary oxides [25,26].

The curves of thermally stimulated luminescence (TSL) were registered for a spectrally integrated (1.9−4.1 eV) signal or the emission selected by an optical filter by means of a Harshaw Model 3500 TLD Reader under sample heating with a constant rate of β = 2 K/s in the atmosphere of flowing nitrogen. Irradiation of the samples with X-rays was performed using a tungsten tube operated at 40 kV and 10 mA, approximate absorbed dose was 1.5 kGy.

3. Results and discussion

Fig. 1 demonstrates the spectrum of RIOA measured in a wide spectral region at RT for a fast-neutron-irradiated α-Al_2O_3 single crystal with a thickness of d = 0.09 mm. According to the existing literature data [7-12], the dominant band around 6 eV (the OD maximum is located at I_{max} = 6.03 eV) is ascribed to the neutral F centers; the charged F^+ centers are responsible for two RIOA bands with I_{max} = 5.33 eV and I_{max} = 4.82 eV, while three significantly less intense absorption bands (see left ordinate scale) are connected with oxygen divacancies, F_2 dimers in different charge states − F_2, $F_2^+$and F_2^{2+}centers. Because of rather low absorbance

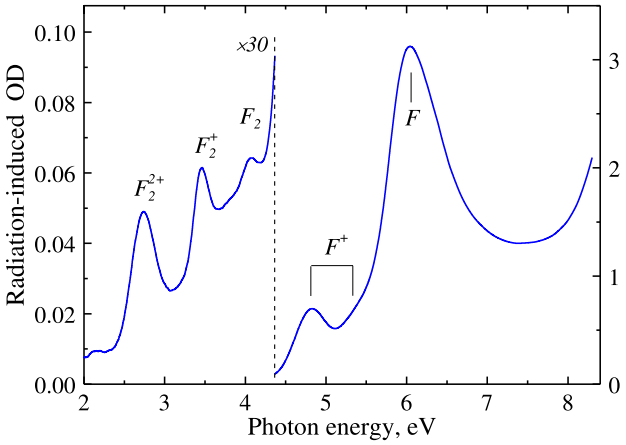

Fig. 1. The spectrum of RIOA measured at RT for an Al_2O_3 single crystal irradiated with fast neutrons ($\Phi = 6.9 \times 10^{18}$ cm^{-2}, RT, d = 0.09 mm).

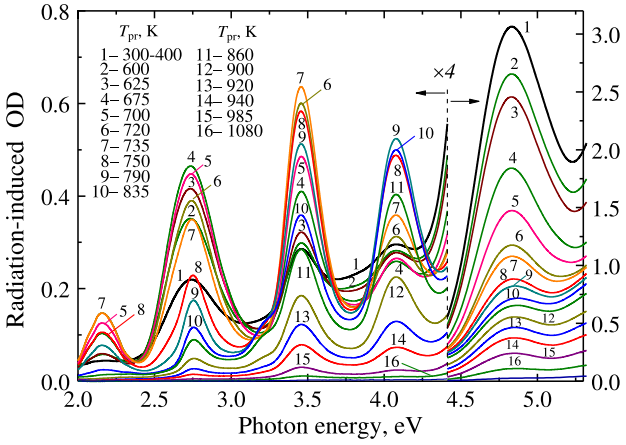

Fig. 2. Spectra of RIOA for an Al_2O_3 single crystal with d = 0.37 mm after irradiation with fast neutrons ($\Phi = 6.9 \times 10^{18}$ cm^{-2}, RT, curve 1) or additional preheating to different temperatures T_{pr}. All spectra are measured at RT.

(low OD values) of the F_2-type dimers, a left part of RIOA spectrum in Fig. 1 is multiplied by a factor of 30. Consequently, further results related to dimer centers belong to a thick irradiated sample with d = 0.37 mm. The concentration of the F^+ centers in our irradiated Al_2O_3 crystals was determined to be close to 1×10^{18} cm^{-3} using the Smakula-Dexter formula for the corresponding RIOA bands or by means of the Bruker programs on the basis of the EPR signal of paramagnetic F^+ centers.

Additional information on the microstructure and nature of lattice defects can be obtained by studying the radiation damage recovery by means of a following thermal annealing of the irradiated crystal. It should be stressed that the structural defects of "radiation-induced origin" (i.e. related to novel Frenkel pairs formed under irradiation) undergo irreversible annealing and do not reappear after additional irradiation of a totally annealed crystal by X-rays at RT. On the other hand, the reappearance of a certain structural defect after additional X-irradiation indicates that we are dealing with some kind of as-grown defects. In wide-gap metal oxides, X-rays do not create new structural defects, but generate charge carriers which can be trapped at effective traps – as grown defects or impurity ions. Note that single and dimer F-type centers under consideration are undoubtedly the radiation-induced defects.

Fig. 2 presents a set of the RIOA spectra measured at 2.0-5.6 eV for an α-Al_2O_3 crystal after neutron irradiation (curve 1) or additional multiple preheatings to certain T_{pr} up to 1200 K. All spectra

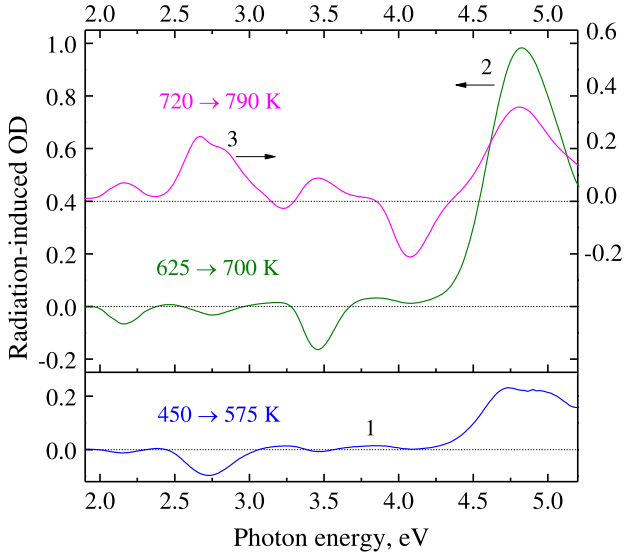

Fig. 3. Difference spectra representing the decrease of RIOA due to the preheating of the neutron-irradiated Al_2O_3 single crystal ($\Phi = 6.9 \times 10^{18}$ cm^{-2}, RT, $d = 0.37$ mm) from 450 to 575 K (curve 1); 625 → 700 K (curve 2) and 720 → 790 K (curve 3).

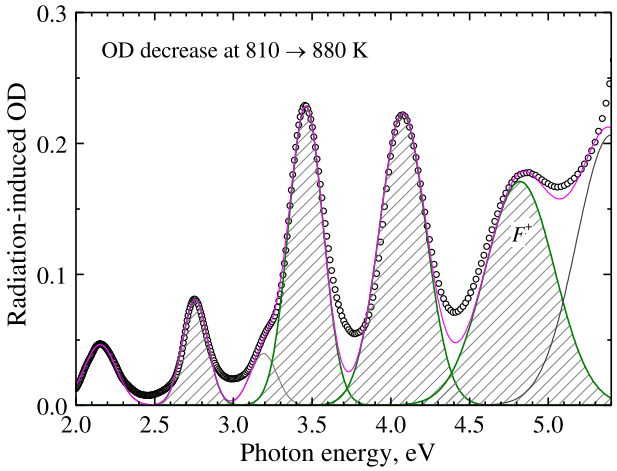

Fig. 4. The difference spectrum representing the decrease of RIOA due to the preheating of the neutron-irradiated Al_2O_3 single crystal ($\Phi = 6.9 \times 10^{18}$ cm^{-2}, RT, $d = 0.37$ mm) from 810 to 880 K (curve with symbols, ooo); the Gaussian decomposition components of this curve (the areas of the main components under consideration are shaded) and their sum (thin solid line).

are measured at RT, while some of the spectra with inconsequential changes in intensity are omitted in Fig. 2. For the irradiated crystal with used thickness of $d = 0.37$ mm, only a low-energy band of the F^+ centers fits the measuring limits of OD values. Even a cursory examination of the figure points to the complexity of temperature behavior of different F_2-type dimers. The last circumstance becomes even more evident when considering the changes of RIOA in different temperature regions.

The difference spectra representing the RIOA decrease due to subsequent preheatings from $T_{pr}(1)$ to $T_{pr}(2)$ are shown in Fig. 3. The regions with negative OD values illustrate the temperature ranges where a certain absorption band (and the corresponding defect concentration) increases. Note that the enhancement of different RIOA bands ascribed to the F_2 dimers in different charge states occurs in different temperature regions. At first, the rise of the F_2^{2+}centers (~2.75 eV band) takes place at 450→575 K; the subsequent preheating of the irradiated sample from 625 to 700 K is accompanied by the rise of the F_2^+band peaked at ~3.45 eV, while, finally, the temperature region of 720-790 K corresponds to the increase of the F_2 center concentration (RIOA band peaked at ~4.1 eV). Note that the decrease of the F^+ center concentration (estimated via RIOA band at ~4.8 eV) is clearly seen for all three temperature ranges presented in Fig. 3.

In order to analyze more precisely the thermal annealing/transformation of different F_2-type centers, we used the decomposition of RIOA into elementary Gaussian components, each of which serves as a measure of a certain type of radiation defects – a concentration of the corresponding radiation defects can be estimated via the integrated area S or the Gaussian peak intensity (OD at I_{max}). Recently, the similar decomposition procedure was successfully used for the investigation of the processes of accumulation and subsequent thermal annealing of different single F-type defects in MgO single crystals exposed to irradiation with swift Xe-ions [26,27]. Note that the result important from methodological point of view was obtained for MgO in Refs. 26 and 27 – the estimation of defect concentration via S and OD at I_{max} for Gaussians or even via OD value at photon energy with dominant contribution of a certain defect type (but without decomposition) leads to practically identical results.

Fig. 4 presents the decomposition into Gaussians of a difference spectrum representing the decrease of RIOA due to the preheating of the neutron-irradiated Al_2O_3 crystal ($d = 0.37$ mm) from 810 to 880 K. We tried to limit the formal decomposition by a minimum number of components including those ascribed in the literature to F_2,$F_2^+$and F_2^{2+}centers – I_{max} at 4.07 eV (FWHM of 0.35 eV), 3.45 (0.26) and 2.75 (0.19) eV, respectively. Consequently, the sum of Gaussians does not fit perfectly to the experimental curve in the overlapping regions of elementary band wings. The used region of 810-880 K corresponds to temperatures when mutual transformations between different F_2 dimers are completed and a synchronous attenuation of all RIOA bands related to single or dimer F-type centers takes place (see further text related to Fig. 7).

In addition, a neutron-induced background after preheating to high T_{pr} is rather low as well, while such background significantly complicates the analysis of the RIOA spectra after preheatings to lower T_{pr} (see Fig. 1). The similar temperature behavior of the background mainly caused by the scattering loss was earlier considered in neutron-irradiated MgO [28] or ~GeV-ion-irradiated complex metal oxides (see, e.g., [29]). In case of rather low values of OD in heavily irradiated materials, it is rather difficult to separate a real RIOA and light scattering on large-size radiation damage. As a result, the extinction spectra are measured in similar cases.

The enhanced neutron-irradiation-induced background in α-Al_2O_3 crystals is responsible for even more significant mismatch between the experimental RIOA curves, measured straight after irradiation or preheatings to lower values of T_{pr}, and the decomposition results just in the photon energy regions between the band maxima. On the other hand, the effect of light scattering is negligible and independent on T_{pr} for the spectral region responsible for the F^+ centers – the RIOA band peaked at ~4.8 eV is characterized by significantly higher OD values. In the present study, the constant shapes of Gaussians connected with F_2, $F_2^+$and F_2^{2+}centers, respectively (they are shown in Fig. 4) were used for the annealing kinetic analysis in the whole temperature range of 300-1100 K. The RIOA spectra have been measured and decomposed into Gaussian components always at the same temperature, RT and, therefore, S or I_{max} parameters of a Gaussian obtained after each preheating and connected with a certain type of dimer centers are proportional to the concentration of the corresponding defects. Although the oscillator strength values f for dimer-related bands are

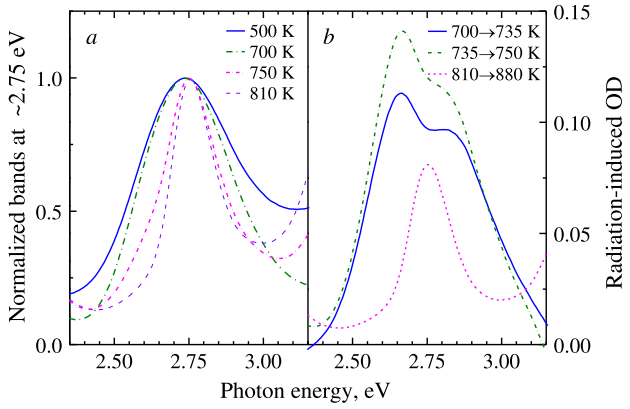

Fig. 5. *a* – Normalized shapes of the ~2.75-eV band measured for a neutron-irradiated Al_2O_3 single crystal after preheating to different T_{pr}. *b* - Difference spectra representing the decrease of RIOA due to the preheating of the neutron-irradiated sample from $T_{pr}(1)$ to $T_{pr}(2)$.

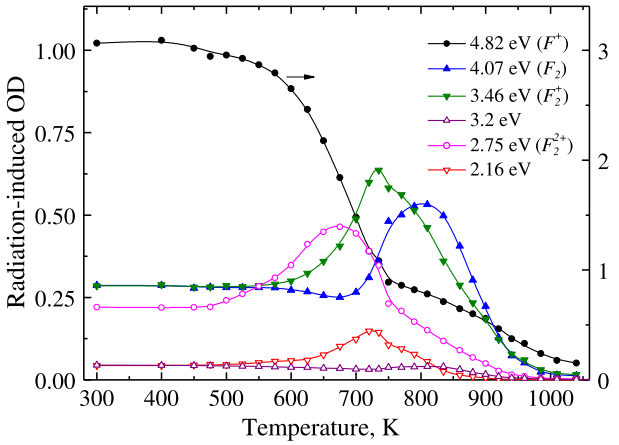

Fig. 6. Dependences of the RIOA related to certain Gaussian components (at I_{max}) on the preheating temperature for a neutron-irradiated Al_2O_3 single crystal ($\Phi = 6.9 \times 10^{18}$ cm^{-2}, RT, $d = 0.37$ mm). Right ordinate belongs only to F^+ centers.

unknown, the experimentally measured annealing curve displays real changes of the certain defect concentrations with T_{pr}; and the lowest limit of the defect concentration could be roughly estimated by the Smakula-Dexter formula with $f = 1$. As it was mentioned earlier, the concentration of the F^+ centers in our samples is about 10^{18} cm^{-3}, and the estimated amount of the F_2 dimers, approximately 10^{17} cm^{-3}, exceeds with enough the impurity/as-grown defect concentration in non-doped samples.

Note that the band at ~2.75 eV was earlier characterized in the literature by a bandwidth of about 0.3 eV [9,11], while our decomposition gives smaller value of FWHM, ~0.19 eV. Fig. 5 clearly demonstrates the complexity of this RIOA band, which tentatively consists of several elementary components, the annealing of which occurs in different temperature regions. Fig. 5*a* shows the normalized band shapes measured at RT after preheatings of the neutron-irradiated sample to different T_{pr}, the bandwidth significantly decreases with preheating temperature. According to the difference spectra (Fig. 5*b*), at least two components are visible in the spectral region under consideration at 700-750 K, while a single narrow component with the maximum at 2.75 eV and practically constant bandwidth remains in the sample after preheatings above $T_{pr} = 750$ K. Just this elementary band corresponds, in our opinion, to F_2^{2+}centers, the thermal annealing of which as well as their transformation into other types of F_2 dimers is the purpose of the present study. However, the annealing curve constructed on the basis of only one narrow component simplifies to some degree the real temperature behavior of the RIOA around 2.75 eV. Other types of F_2-dimers can be sufficiently accurately characterized by elementary Gaussians presented in Fig. 4.

Fig. 6 shows the annealing kinetics of single and dimer *F*-type centers for a neutron-irradiated Al_2O_3 single crystal with $d = 0.37$ mm. The value of I_{max} for a certain Gaussian is taken as a concentration of the corresponding radiation-induced defects. Because of low intensity of the 3.2 eV band (shoulder) and relatively high scattering background that impedes justified decomposition after low T_{pr}, the measured values of RIOA were taken for the construction of the respective annealing curve. In contrast to a continuous decrease of the number of the F^+ centers in a whole temperature region from ~450 to 1050 K, the temperature dependences for the concentration of dimer centers are more complicated and contain increasing stages, although in different temperature regions. The F_2^{2+}center concentration starts to rise first above 500 K and reaches its maximum value around 675 K; a significant increase in the number of the F_2^+centers occurs from 675 up to 735 K; while the maximum concentration of the F_2 centers is achieved at even

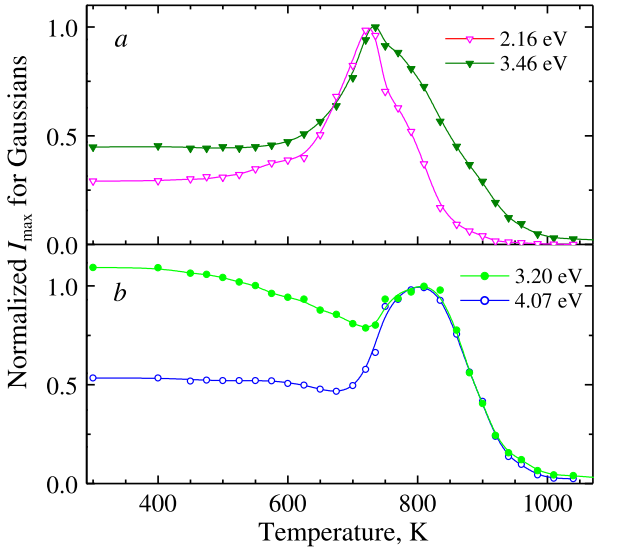

Fig. 7. Normalized dependences of the I_{max} for certain Gaussian components on the preheating temperature in a neutron-irradiated Al_2O_3 crystal with $d = 0.37$ mm.

higher temperature, around 800 K. Note that the rise of absorption bands related to F_2-type dimers (for some components or without specification) was already reported in [6,9,12].

Before discussing the mechanisms of mutual transformation of dimer centers in different charge states, let us consider the origin of two other RIOA bands clearly attending in Figs. 3 and 4 – these are the band with I_{max} at 2.16 eV and a shoulder at $I_{max} = 3.2$ eV. According to the data in Fig. 7, there is clear correlation in behavior of two pairs of the RIOA bands. The temperature dependencies of the bands peaked at 2.16 and 3.46 eV as well as at 3.20 and 4.07 eV are very similar and the increase of these bands above 700 K takes place simultaneously. Especially impressive is the coincidence of the increasing stages in Fig. 7*b*, although the real OD values for the 3.2-eV band (i.e., the corresponding center concentration) are rather low (see Fig. 6). Therefore, it is reasonable to suggest the same origin for the RIOA bands demonstrating the similar dependence – the shoulder at 3.2 eV could be attributed to neutral (with respect to a regular lattice) F_2 centers, while the 2.16 eV band could be considered as the second band of the F_2^+centers. The assignment of two (sometimes even three) bands to the same center, usually with molecular or complex/aggregate structure, is common in the literature (see, e.g., [30-32]). Note that the bands

at 2.75 and 2.17 eV have been already attributed to the F_2^+centers in Ref. 8, mainly on the basis of their behavior under X-rays or UV-irradiation. However, this suggestion contradicts to the annealing kinetics investigated in the present study.

It is generally accepted that the annealing of the single *F*-type centers in neutron-irradiated metal oxides is due to the recombination of the becoming mobile oxygen interstitials with still immobile anion vacancies that are part of the F^+ and *F* centers, while the thermal annealing of the *F* and F^+ absorption bands in additively colored corundum, not containing anion interstitials, takes place at significantly higher temperatures, above 1300 K [7,8,11,17]. Accordingly, the data depicted in Fig. 6 illustrate the annealing at 500-1000 K of complementary Frenkel defects, vacancy-interstitial pairs created by fast fission neutrons via the universal collision mechanism. Note that only the F^+ centers are measurable in our thick sample, although the similar annealing kinetics is valid for the *F* centers in neutron-irradiated Al_2O_3 crystals as well. The precise analysis of the annealing kinetics of single *F*-type centers (measured via optical absorption or the EPR method) and its simulation in terms of diffusion-controlled reactions will be presented in a separate forthcoming paper.

The decay of dimer centers at high temperatures could be also explained via the filling of anion vacancies comprising F_2-type centers by oxygen interstitials still remaining up to high temperatures in the form of some associations/aggregates, more stable than single anion interstitials (complementary defects for the single *F* and F^+ centers). On the other hand, the increasing stages in the annealing kinetics of the F_2-type centers (Figs. 6 and 7) should be explained as well. Note that if the transformations $F_2^{2+} \rightarrow F_2^+ \rightarrow F_2$at constantly growing T_{pr}, 700→ 750 K could be, in general, attributed to the recharging of dimers by the electrons emerging in the corresponding temperature regions, then the involvement of a some aggregation mechanism is needed to explain the concentration rise of the F_2^{2+}centers, which was detected at lower temperatures, 500-650 K.

It was mentioned already that single *F* and F^+ centers are immobile in corundum below 1300 K. At the same time, one can expect the mobility of an oxygen vacancy (not associated with one/two electrons, i.e. F^{2+}) at lower temperatures. It is noteworthy that similar situation is typical of alkali halides, where a single-charged (empty, without a trapped electron) anion vacancy, named also as an α center, becomes mobile around RT, while the *F* centers are immobile at least up to 400 K (see, e.g. [33] and references therein). Just the migration/diffusion of a fluorine vacancy toward the *F* center and the subsequent trapping of an additional electron is used in explaining the formation of the F_2 (M) centers at RT in LiF via the following reactions: $F^+(\alpha) + F \rightarrow F_2^+$; $F_2^+ + e \rightarrow F_2$[34-36]. In our opinion, an oxygen vacancy (F^{2+}) tentatively becoming mobile above 500 K interacts with an *F* center causing the formation of an F_2^{2+}center in α-Al_2O_3 crystals.

Further heating of the neutron-irradiated corundum causes the transformation $F_2^{2+} \rightarrow F_2^+ \rightarrow F_2$, tentatively, by the recharging of dimer centers via consecutive trapping of two electrons. We tried to clear up a source of charge carriers in high-temperature region by studying the thermally stimulated luminescence of irradiated α-Al_2O_3crystals. Fig. 8*a* shows the TSL curves measured for a spectrally integrated signal at the heating of a neutron-irradiated sample with a constant rate of $\beta = 2$ K/s up to 853 K (heater-related background is subtracted). Because of rather fast drop of temperature after reaching 853 K in the used TLD reader, only a small part of defects responsible for the TSL at such high temperatures becomes annealed. Two measurements were performed one after another for the same sample (curves 1 and 2) demonstrating the presence of a high-temperature TSL peak, which is rather intense and could not be eliminated via fast preheatings to 853 K – the limit of the setup used. Nevertheless, the difference of these two sequentially measured TSL curves contains clear manifestations of the peak maximum around 840 K (see curve 3).

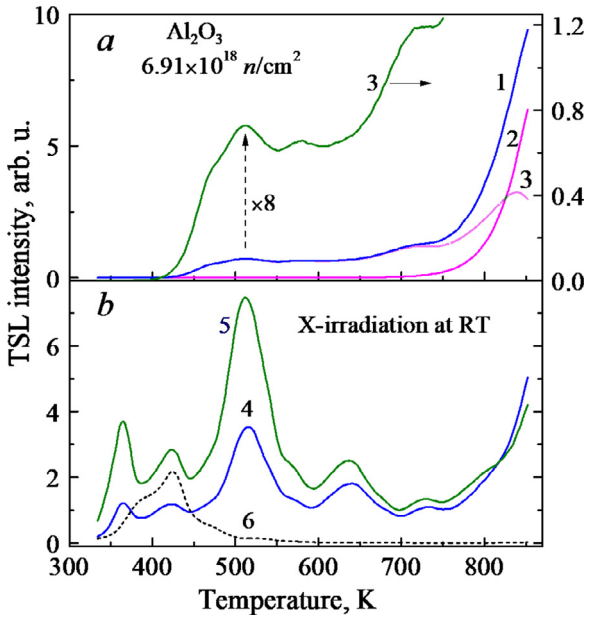

Fig. 8. TSL curves measured for a spectrally integrated signal with a constant heating rate of $\beta = 2$ K/s up to 853 K (experimental limit). *a* – two successive measurements for the same neutron-irradiated sample (curves 1 and 2) and the difference of these curves – curve 3 (multiplied by a factor of 8 as well). *b* – Before the next measuring the sample was additionally exposed to X-rays at RT (curves 4 and 5). TSL measured after total annealing of the neutron-irradiated crystal to 1300 K and additional exposure to X-rays at RT (curve 6). The X-ray dose, ~1.5 kGy was the same for all cases (curves 4 to 6).

After the second preheating of the neutron-irradiated α-Al_2O_3 to 853 K, the sample was additionally exposed to X-rays at RT and the TSL curve was measured once more (curve 4). According to Fig 8*b*, this curve contains several low-temperature peaks, the intensity of which even increases after repeated isodose X-irradiation at RT (curve 5). Note that high-temperature TSL continuously decreases with each preheating (TSL measuring) procedure. Just this high-temperature peak is the source of charge carriers becoming retrapped and manifesting themselves via low-temperature peaks. In case of sample preheating to 700 K, i.e. below the beginning of ~840 K TSL peak, the reversible appearance of low-temperature peaks with practically the same intensity is detected after repeated isodose X-irradiation at RT. On the other hand, TSL above 500 K is totally absent after X-irradiation of the neutron-irradiated sample preliminarily annealed to 1300 K (curve 6). Therefore, the high-temperature TSL is definitely connected with the structural defects induced by fast neutrons, the thermal destruction of which ensures the release of electrons needed for the retrapping of the $F_2^{2+}$and F_2^+centers.

Earlier, thermoluminescent characteristics have been extensively studied in nominally pure Al_2O_3 single crystals (see [37] and references therein) as well as dosimetric (anion deficient) Al_2O_3:C [3,4] exposed to various types of ionizing radiation (UV-light, X- or gamma-rays), which is unable to produce structural damage in α-Al_2O_3. In these studies, only TSL up to ~600 K, i.e. below the beginning of the recharging processes of the F_2 centers, were detected. On the other hand, only episodic studies of TSL have been performed in pure α-Al_2O_3 exposed to particle irradiation (neutrons, energetic ions and electrons) [16,39,40]. In particular, irradiation with mainly thermal neutrons [39] or fast neutrons at 20 K [39] leads to the appearance of TSL peaks significantly below the high-temperature one detected after crystal irradiation by fast fis-

sion neutrons in the present study (see Fig. 8*a*), while the peaks are rather similar to those detected after additional X-irradiation of our samples (Fig. 8*b*). Note that ~700 K was a technical limit for a TSL setup used in Ref. 16 for the measurements for heavy-ion-irradiated corundum crystals. In our opinion, the TSL above 700 K detected in the present study can be related to the transformation processes with the F_2-type centers according to the above-suggested scenario. This conclusion is partly supported by the presence of deep charge traps (~840 K) in Al_2O_3:C that contain significant concentration of as-grown *F*- and F_2-type defects.

Similar to alkali halides (so-called α-*I* and *F*-*H* pairs of Frenkel defects [23]), both neutral and charged vacancy-interstitial Frenkel pairs are formed in α-Al_2O_3 under fast neutron irradiation. Bimolecular type of recombination between *F*, F^+ and mobile complementary oxygen interstitials (in neutral or charged state) is responsible for the thermal annealing of single *F*-type defects. It is important to note that the concentration of the neutral *F* centers in our samples is higher than that for charged F^+ ones. Moreover, the annealing of the *F* centers, being very similar to that of the F^+ centers, starts at slightly higher temperatures (up to 50 K, see our forthcoming paper). As a result, the tentative recombination of a charged anion interstitial with an *F* center leads to the release of an electron able to participate in the recharging of dimer centers in corundum.

4. Conclusions

In addition to single F^+ and *F* centers, the F_2-type dimer centers in different charge states are also formed under irradiation of α-Al_2O_3 single crystals with fast fission neutrons via the collision mechanism of radiation damage. In contrast to the continuously decreasing thermal annealing kinetics of single *F*-type centers due to their recombination with becoming mobile oxygen interstitials, the temperature dependences of the concentration of different dimer centers (estimated via decomposition of radiation-induced absorption into elementary Gaussians) on preheating temperature contain increasing stages above ~550 K. In our opinion, the concentration rise of the F_2^{2+}centers up to 650 K could be explained by the mobility of an oxygen vacancy (not associated with one/two electrons) above ~500 K, while mutual transformation of dimers $F_2^{2+} \rightarrow F_2^{+} \rightarrow F_2$at 675-735 and 750-800 K, respectively is caused by the recharging of dimers via consecutive trapping of two electrons. High temperature TSL detected in our samples confirms the release of charge carriers in the temperature region under consideration. Nevertheless, the clarification of the origin of high-temperature TSL peaks in fast neutron irradiated α-Al_2O_3 single crystals should be continued.

Credit Author Statement

Author's contribution

E. Shablonin: optical absorption, thermal annealing, TSL measurements

A.I. Popov: Conceptualization, writing.

G. Prieditis: data analysis.

E. Vasil'chenko: Sample preparation, technical guidance.

A. Lushchik: Conceptualization, writing.

Declaration of Competing Interest

The authors declare that they have no known competing financial interests or personal relationships that could have appeared to influence the work reported in this paper.

Acknowledgements

This work has been carried out within the framework of the EUROfusion Consortium and has received funding from the Euratom research and training programme 2014-2018 and 2019-2020 under grant agreement No 633053. The views and opinions expressed herein do not necessarily reflect those of the European Commission. In addition, the research leading to these results has received funding from the Estonian Research Council grant (PUT PRG619).

References

[1] S.J. Zinkle, C. Kinoshita, Defect production in ceramics, J. Nucl. Mat. 251 (1997) 200–217.
[2] S.M. Gonzales de Vicente, E.R. Hodgson, T. Shikama, Functional materials for tokamak in-vessel systems – status and applications, Nucl. Fusion 57 (2017) 092009.
[3] D.A. Blokhin, V.M. Chernov, I. Blokhin, Nuclear and physical properties of dielectrics under neutron irradiation in fast (BN-600) and fusion (DEMO-S) reactors, Phys. Atom. Nuclei 80 (2017) 1279–1284.
[4] S.W.S. McKeever, M.S. Akselrod, L.E. Colyott, N. Agersnap Larsen, J.C. Polf, V.H. Whitley, Characterisation of Al_2O_3 for use in thermally and optically stimulated luminescence dosimetry, Radiat. Prot. Dosim. 84 (1999) 163–168.
[5] S.V. Nikiforov, A. Lushchik, V. Nagirnyi, I. Romet, A.I. Ponomareva, D.V. Ananchenko, E.V. Moiseykin, Validation of the model of TSL isothermal decay in dosimetric α-Al_2O_3 crystals, Radiat. Meas. 122 (2019) 29–33.
[6] G.P. Pells, Radiation damage effects in alumina, J. Am. Ceram. Soc. 77 (1994) 368–377.
[7] B.D. Evans, A review of the optical properties of anion lattice vacancies, and electrical conduction in α-Al_2O_3: their relation to radiation-induced electrical degradation, J. Nucl. Mater. 219 (1995) 202–223.
[8] K.H. Lee, J.H. Crawford, Additive coloration of sapphire, Appl. Phys. Lett. 33 (1978) 273–275.
[9] K. Atobe, N. Nishimoto, M. Nakagawa, Irradiation-induced aggregate centers in single crystal $A1_2O_3$, Phys. Stat. Solidi A 89 (1985) 155–162.
[10] B.D. Evans, G.J. Pogatshnik, Y. Chen, Optical properties of lattice defects in α-Al_2O_3, Nucl. Instrum. Meth. B 91 (1994) 258–262.
[11] R. Ramírez, M. Tardío, R. Gonz_alez, J.E. Mu~noz Santiuste, M.R. Kokta, Optical properties of vacancies in thermochemically reduced Mg-doped sapphire single crystals, J. Appl. Phys. 101 (2007) 123520.
[12] M. Izerrouken, T. Benyahia, Absorption and photoluminescence study of Al_2O_3 single crystal irradiated with fast neutrons, Nucl. Instrum. Meth. B 468 (2010) 2987–2990.
[13] V.A. Skuratov, K.J. Gun, J. Stano, D.L. Zagorski, In situ luminescence as monitor of radiation damage under swift heavy ion radiation, Nucl. Instrum. Meth. B 245 (2006) 194–200.
[14] A. Lushchik, Ch. Lushchik, K. Schwartz, F. Savikhin, E. Shablonin, A. Shugai, E. Vasil'chenko, Creation and clustering of Frenkel defects at high density of electronic excitations in wide-gap materials, Nucl. Instrum. Meth. B 277 (2012) 40–44.
[15] C. Grygiel, F. Moisy, M. Sall, H. Lebius, E. Balanzat, T. Madi, T. Been, D. Marie, I. Monnet, In-situ kinetics of modifications induced by swift heavy ions in Al_2O_3: Colour centre formation, structural modification and amorphization, Acta Mater 140 (2017) 157–167.
[16] J.M. Costantini, Y. Watanabe, K. Yasuda, M. Fasoli, Cathodo-luminescence of color centers induced in sapphire and yttria-stabilized zirconia by high-energy electrons, J. Appl. Phys. 121 (2017) 153101.
[17] A.I. Popov, A. Lushchik, E. Shablonin, E. Vasil'chenko, E.A. Kotomin, A.M. Moskina, V.N. Kuzovkov, Comparison of the F-type center thermal annealing in heavy-ion and neutron irradiated Al_2O_3 single crystals, Nucl. Instrum. Meth. B 433 (2018) 93–97.
[18] V.N. Kuzovkov, E.A. Kotomin, A.I. Popov, Kinetics of the electronic center annealing in Al_2O_3 crystals, J. Nucl. Mater. 502 (2018) 295–300.
[19] Yu.F. Zhukovskii, A. Platonenko, S. Piskunov, E.A. Kotomin, Ab initio simulations on migration paths of interstitial oxygen in corundum, Nucl. Instrum. Meth. B 374 (2016) 29–34.
[20] R.A. Evarestov, A. Platonenko, D. Gryaznov, Y.F. Zhukovski, E.A. Kotomin, First-principles calculations of oxygen interstitials in corundum: a site symmetry approach, Phys. Chem. Chem. Phys. 19 (2017) 25245.
[21] A. Platonenko, D. Gryaznov, Y.F. Zhukovskii, E.A. Kotomin, Ab initio simulations on charged interstitial oxygen migration in corundum, Nucl. Instrum. Meth. B 435 (2018) 74–78.
[22] N. Itoh, D.M. Duffy, S. Khakshouri, A.M. Stoneham, Making tracks: electronic excitation roles in forming swift heavy ion tracks, J. Phys.: Condens. Matter 21 (2009) 474205.
[23] A. Lushchik, Ch. Lushchik, A.I. Popov, K. Schwartz, E. Shablonin, E. Vasil'chenko, Influence of complex impurity centres on radiation damage in wide-gap metal oxides, Nucl. Instrum. Meth. B 374 (2016) 90–96.
[24] Ch. Lushchik, A. Lushchik, Evolution of anion and cation excitons in alkali halide crystals, Fiz. Tverd. Tela 60 (2018) 1478–1494 [Phys. Solid State 60 (2018) 1487-1505].

[25] G. Baubekova, A. Akilbekov, E.A. Kotomin, V.N. Kuzovkov, A.I. Popov, E. Shablonin, M. Zdorovets, E. Vasil'chenko, A. Lushchik, Thermal annealing of radiation damage caused by swift ^{132}Xe ions in MgO single crystals, Nucl. Instrum. Meth. B 462 (2020) 163–168.
[26] A. Lushchik, S. Dolgov, E. Feldbach, R. Pareja, A.I. Popov, E. Shablonin, V. Seeman, Creation and thermal annealing of structural defects in neutron-irradiated $MgAl_2O_4$ single crystals, Nucl. Instrum. Meth. B 435 (2018) 31–37.
[27] G. Baubekova, A. Akilbekov, E. Feldbach, R. Grants, I. Manika, A.I. Popov, K. Schwartz, E. Vasil'chenko, M. Zdorovets, A. Lushchik, Accumulation of radiation defects and modification of micromechanical properties under MgO crystal irradiation with swift Xe ions, Nucl. Instrum. Meth. B 463 (2020) 50–54.
[28] R. Gonzalez, Y. Chen, R.M. Sebek, G.P. Williams Jr., R.T. Williams, W. Gellermann, Properties of the 800-nm luminescence band in neutron-irradiated magnesium oxide crystals, Phys. Rev. B 43 (1991) 5228–5233.
[29] A. Lushchik, Ch. Lushchik, V. Nagirnyi, S. Pazylbek, O. Sidletskiy, K. Schwartz, E. Shablonin, A. Shugai, E. Vasil'chenko, On the mechanisms of radiation damage and prospects of their suppression in complex metal oxides, Phys. Status Solidi B 250 (2013) 261–270.
[30] E.A. Kotomin, A. Stashans, L.N. Kantorovich, A.I. Lifshitz, A.I. Popov, I.A. Tale, J.-L. Calais, Calculations of the geometry and optical properties of F_{Mg} centers and dimer (F_2-type) centers in corundum crystals, Phys. Rev. B 51 (1995) 8770–8778.
[31] S. Sanyal, M.S. Akselrod, Anisotropy of optical absorption and fluorescence in Al_2O_3:C,Mg crystals, J. Appl. Phys. 98 (2005) 033518.
[32] S. Ikeda, T. Uchino, Temperature and excitation energy dependence of the photoionization of the F_2 center in α-Al_2O_3, J. Phys. Chem. C 118 (2014) 4346–4353.
[33] Eds E. Sonder, W.A. Sibley, J.H. Crawford, L.M. Slifkin (Eds.) Plenum Press, New-York, 1972. EdsChap. 4.
[34] Y. Farge, M. Lambert, R. Smoluchowski, Mechanisme de fotmation des centres M et R, Solid State Commun 4 (1966) 333–336.
[35] J. Nahum, Optical properties and mechanism of formation of some F-aggregate centers in LiF, Phys. Rev. 158 (1967) 814–825.
[36] A. Dauletbekova, K. Schwartz, M.V. Sorokin, J. Maniks, A. Rusakova, M. Koloberdin, A. Akilbekov, M. Zdorovets, LiF crystals irradiated with 150 MeV Kr ions: Peculiarities of color center creation and thermal annealing, Nucl. Instrum. Meth. B 295 (2013) 89–93.
[37] G.P. Summers, Thermoluminescence in single crystal α-Al_2O_3., Radiat. Prot. Dosim. 8 (1984) 69–80, doi:10.1093/oxfordjournals.rpd.a083043.
[39] Abu Zayed Mohammad Saliqur Rahman, T Kobayashi, T Awata, K Atobe, Thermoluminescence of α-Al_2O_3 by neutron irradiation at low temperature, Radiat. Eff. Defect. Solids 165 (2010) 290–297, doi:10.1080/10420150903481509.
[40] M. Kulkarni S., N. Rawat S., S. Thakare V., K. Jagadeesan C., D. Mishra R., K. Muthe P., B. Bhatt C., S. Gupta K., D. Sharma N., TL and OSL studies on neutron irradiated pure α-Al_2O_3 single crystals, Radiat. Meas. 46 (2011) 1704–1707, doi:10.1016/j.radmeas.2011.04.028.

Institute of Solid State Physics, University of Latvia as the Center of Excellence has received funding from the European Union's Horizon 2020 Framework Programme H2020-WIDESPREAD-01-2016-2017-TeamingPhase2 under grant agreement No. 739508, project CAMART²